UNIVERSITY OF BIRMINGHAM

The extraction of NdFeB magnets from automotive scrap rotors using hydrogen

Jonsson, Christian; Awais, Muhammad; Pickering, Lydia; Degri, Malik; Zhou, Wei; Bradshaw, Andrew; Sheridan, Richard; Mann, Vicky; Walton, Allan

Link to publication on Research at Birmingham portal

The extraction of NdFeB magnets from automotive scrap rotors using hydrogen

Christian Jönsson, Muhammad Awais*, Lydia Pickering, Malik Degri, Wei Zhou, Andy Bradshaw, Richard Sheridan, Vicky Mann, and Allan Walton

School of Metallurgy and Materials, University of Birmingham, B15 2TT Edgbaston, UK

*Corresponding author: M.Awais@bham.ac.uk

Abstract

Scrap containing NdFeB is a valuable resource for the production of NdFeB magnets as the demand for these materials grows. One of the challenges is to recover the rare earths or the NdFeB alloy powder in a clean and cost effective manner so that it can be re-processed into new magnets rather than becoming lost to landfill. Work on using hydrogen to process scrap magnets (HPMS) has been shown to be successful when targeting hard disk drives. Currently, there is a lack of information on reliable methods to separate out NdFeB from other scrap sources such as automotive drives. In the near future, with increasing sales and electrification of cars, the automotive sector could be an important source for Dy containing magnets. In this paper, the hydrogen processing of scrap magnets has been demonstrated as an extraction method for NdFeB from automotive rotors for the first time, with the aim to examine the viability of this recycling process and learn lessons for design for recycling. Thus leading to the sustainable production of these components. Significant challenges were outlined when applying the hydrogen process to rotors with embedded magnets. After the extraction, further process steps may also be needed to separate epoxy coatings, as sieving could only reduce the carbon content to 1420 ppm, compared to 770 ppm in the base alloy. The gravimetric measurements also confirmed that Dy additions increase both the initiation and absorption time for hydrogen decrepitation. Hence, a higher hydrogen pressure will be required to speed up the process.

Highlights:

- Hydrogen can be used to extract NdFeB magnets from the automotive rotors, however, many challenges are presented due to rotors being designed without recycling in mind.
- The importance of design choices that have a negative impact on the recycling of automotive rotors are investigated in this work, so can be avoided in future designs.
- Higher Dy additions slow down the kinetics of the hydrogen decrepitation reaction by 75 % at room temperature and 1.2 bar hydrogen pressure.

34   • Scrap magnets with 8.5 wt% Dy took longer to initiate the reaction and a significantly

35   higher hydrogen pressure is required for quick processing of the scrap.

36   • The carbon content could only be reduced to 1420 ppm, compared to 770 ppm in the

37   starting material, by sieving the extracted powder to <45 µm because the epoxy

38   coating is breaking up at a similar rate to the HD powder.

39   **Keywords**

40   Recycling, hydrogen decrepitation, automotive, NdFeB, critical materials

41   **1. Introduction**

42   The rare earth elements (REEs) are defined as critical materials in the EU and the US, due to

43   their high economic importance combined with their supply risk (European Commission, 2017,

44   2014; U.S. Department of Energy, 2011). The rare earth market is, to a large extent, driven by

45   the increasing use of neodymium-iron-boron (NdFeB) magnets, which are employed in

46   electronics, industrial and automotive motors, and wind turbine generators. Recycling of end-

47   of-life NdFeB magnets could be part of the solution to alleviate the supply risks for REEs

48   outside of China. At present, however, less than 1 % of REEs are recycled, due to a lack of

49   incentives, inefficient collection, and technological difficulties (Reck and Graedel, 2012). In a

50   study, Habib et al. revealed that primary supply would be unable to meet the forecasted

51   demand of Nd and Dy by 2050 and recycling is unlikely to close the wide gap between future

52   demand and supply by 2050. This means that a highly accelerated rate of Nd and Dy mining

53   will be required to meet the demand. However, it has been suggested that secondary supply

54   from recycling can meet almost 50 % of the demand in the long term i.e. by 2100 (Habib and

55   Wenzel, 2014). Another study estimates that the recycling of EOL magnets could supply 68

56   % of light REE (Nd and Pr) and 11 % of heavy REE (Dy and Tb) demand of NdFeB magnets

57   by 2030 (Schulze and Buchert, 2016).

58   Automotive scrap has the potential to contain a significant amount of NdFeB typically with

59   increased Dy content. The amount of REEs present in fully electric vehicles varies with the

60   type/model of vehicle. Typically, an EV contains 4-5 kg of REE compared to less than a kilo

61   in a new petrol/diesel car (Alonso et al., 2012). To get a bigger perspective on the potential of

62   recycling of these REE from the electric vehicles, IEA estimated that the EV sales reach would

63   reach 44 million vehicles per year by 2030 (IEA, 2019). If these magnets are recycled

64   efficiently, it can create a parallel supply chain to the primary route. Thus, becoming an

65   important source to meet future demand as highlighted by other researchers (Alonso et al.,

66   2012; Du and Graedel, 2011; Habib and Wenzel, 2014). The key, however, is accessing this

67   material in a cost effective and efficient manner. Work is being carried out to address the issue

68 of the low rates of recycling of these critical materials. The creation of a systematic labelling
69 system that encompasses the key metrics for recycling can enable end users of magnetic
70 parts to select more environmentally friendly designs and can also ensure that the magnet
71 containing products can end up at the correct recycling facility (MaXycle, 2018; Burkhardt; et
72 al., 2019; Burkhardt; et al., 2020).

73 Despite a huge surge in the demand for electric vehicles and their recycling potential, there is
74 not much literature available looking at the viability of recycling NdFeB containing scrap from
75 automotive sources. Therefore, this study is aimed to identify the challenges involved to
76 recover NdFeB magnets from end of life automotive scrap. The work also investigates the
77 viability of recycling automotive rotors using hydrogen and provide feedback for design for
78 recycling.

79 **2. Literature Review**

80 Extraction of NdFeB magnets from end of life vehicles is very labour intensive work. It has
81 been shown to be profitable to dismantle the rotor manually due to the amount of Cu in the
82 windings (Bast et al., 2014). Previously, Walton et al. (2015) presented a recycling process,
83 HPMS (Hydrogen Processing of Magnet Scrap), which uses hydrogen to extract NdFeB
84 magnets from the hard disk drives (HDDs) in the form of demagnetised, hydrogenated alloy
85 powder. The VCM-containing corner was cropped off to concentrate the magnet-containing
86 feed and provide a route out for the NdFeB powder. The cropped corners are distorted to
87 fracture the magnets prior to hydrogen exposure for activation. The corners are then loaded
88 into a porous drum inside the hydrogen reactor, which is subsequently tumbled to liberate the
89 powder from the assemblies. Milling and sieving is performed to remove impurities, especially
90 the Ni coating, before the alloy powder can be reprocessed, for example by sintering into new
91 fully dense magnets. Life Cycle Analysis (LCA) has shown that by producing re-sintered
92 magnets using HPMS, energy usage can be reduced by 88 % compared with primary
93 production (Sprecher et al., 2014)

94 Extracting NdFeB magnets from automotive rotors comes with a different set of challenges
95 compared to that of HDDs. The removal of the motor from a car and then the magnet-bearing
96 rotor is labour intensive work. Moreover, automotive rotors come in a wide range of designs,
97 using different materials, and with the magnets placed in various positions, making it difficult
98 to find a universal method for NdFeB extraction. However, the MORE (MOtor REcycling)
99 project stated that stripping down to rotor/stator level is profitable, even with German labour
100 costs, due to the recovery of Cu from the stator windings (Bast et al., 2014). This did not
101 include the potential value of the recovered NdFeB. One method was developed to punch out

102   buried magnets for reuse and another was to shear off surface mounted magnets. The
103   undamaged magnets could then be reused after removal of the adhesive residues.

104   Automotive scrap has a potentially higher value due to the increase in Dy content. The
105   increase in Dy is required to improve performance at typical operating temperatures (Gauder
106   et al., 1988). The two main phases in the NdFeB type magnet microstructure are rare earth
107   (RE) rich, an alloy predominantly rich in Nd but will contain other rare earths such as Dy. The
108   matrix phase consists of $Nd_2Fe_{14}B$, this is the magnetic phase. The Fe can be substituted for
109   Co and the Nd for other rare earths (Sagawa et al., 1985).

110   During the hydrogen decrepitation reaction, the formation of rare earth hydrides at the grain
111   boundary generates exothermic heat that initiates hydrogen diffusion into interstitial sites of
112   the $Nd_2Fe_{14}B$ matrix phase (Harris et al., 1987). Regarding Dy, it has been shown that, at
113   20bar and room temperature, it takes longer to form a hydride from Dy than from Nd (Hirano
114   et al., 2006) and that the $Dy_2Fe_{14}B$ phase can absorb less hydrogen than its Nd counterpart
115   (Bartolomé et al., 1991). However, Saje et al., (1992) did not see a difference in reaction rate
116   when performing hydrogen decrepitation (1 bar, 20 °C) of the $Nd_{16-x}Dy_xFe_{76}B_8$ (at.%, x = 0-3)
117   alloy with varying Dy content. There is some disagreement as to whether the Dy content of
118   the magnets may affect the hydrogen decrepitation of sintered NdFeB (which the HPMS
119   process is based around), where the grain boundary phase plays a key role for the initiation
120   and propagation of the reaction.

121   After the hydrogen decrepitation, the hydrogenated NdFeB powder needs to be purified to
122   remove all the impurities. This purification process has to be done in an inert atmosphere to
123   avoid oxidation. Various authors have noted that both oxygen and carbon have been shown
124   to have detrimental effects on the sintering process for NdFeB (Lopes et al., 2012; Sasaki et
125   al., 2015; Zakotnik et al., 2009). After this, the powder can be inertly milled to single crystal
126   using the jet mill and sintered to new magnets by following the commercial production route
127   (Malik Degri, 2014).

128

3. Experimental Design

130   To look at the feasibility of extraction of hydrogenated NdFeB from magnetic rotors from
131   automotive scrap, the process was broken down into two separate stages. The first stage, to
132   look at the feasibility of using hydrogen processing of magnet scrap (HPMS) applied to
133   automotive rotors and whether pre-processing of the rotors is required to get the magnets to

134 successfully react with hydrogen at room temperature and 1.5 bar. The second stage was to

135 study the kinetics of the reaction hydrogen with the magnets of different Dy content to assess

136 the influence of Dy on hydrogen decrepitation.

3.1.   Extraction from Rotors

138 Pre-separated discarded rotors, from an unnamed motor company, were used in this study,

139 see Figure 1. The grade was determined to be N42SH and the composition of these magnets

140 was measured to be $Nd_{9.08}Pr_{2.62}Dy_{1.38}Fe_{78.99}Al_{1.06}Nb_{0.17}B_{5.81}$ (atomic %) and traces of Gd

141 0.04 at%, Co 0.71 at%, Cu 0.13 at%, Mn 320 ppm, Si 410 ppm and N 170 ppm. The oxygen

142 and carbon contents were 760 ppm and 690 ppm respectively. These rotors contain ten

143 surface-mounted epoxy-coated magnets on a ferritic steel disk with a diameter of 25 cm. The

144 magnets were either non-, semi- or fully embedded in the thermosetting plastic.
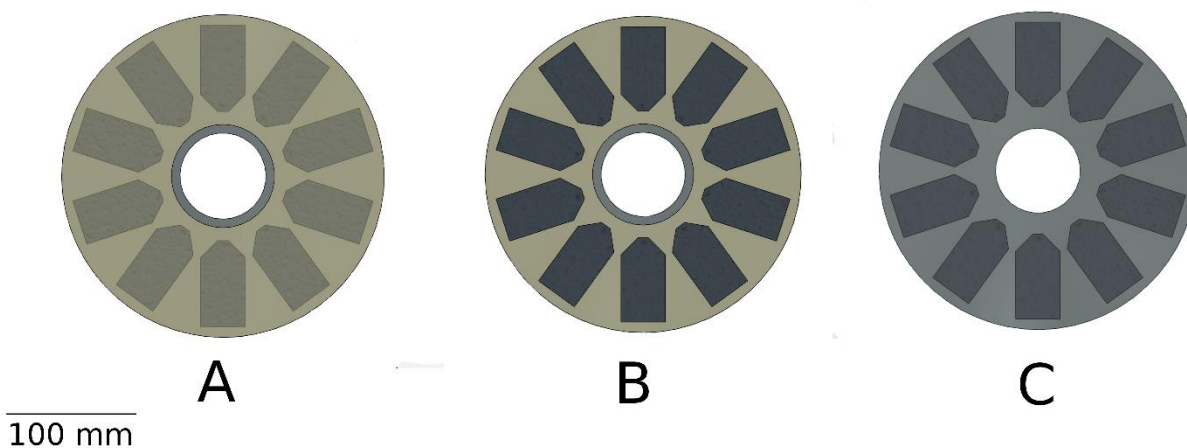

100 mm

A   B   C

Figure 1: A model of the automotive rotors studied in this work, all containing epoxy-coated magnet slots on a
ferritic steel plate. The magnet slots are either a) fully embedded, b) semi-embedded or c) non-embedded in a
thermosetting plastic.

149 The HPMS processing was carried out using a 300 L reaction chamber, shown in Figure 2.

150 The experiments started by loading rotors from the top of the vessel, followed by argon

151 flushing and evacuation to 10^{-2} mbar. Hydrogen was then introduced to a pressure of

152 1.2-1.5 bar in order to initiate the hydrogen decrepitation reaction and the pressure within the

153 vessel was maintained manually throughout the experiment until the pressure had been stable

154 for several hours. All processing was performed at room temperature and the hydrogen was

155 removed at the end of the reaction. The recycling rig provided the option of connecting the

156 argon inlet to a pneumatic spinner that was connected to the assembly holder. As argon is

157 fed, the spinner agitated the assemblies, liberating the NdFeB powder, which would fall into

158   the collection pot. The collection pot was then be sealed by the closing of two ball valves and

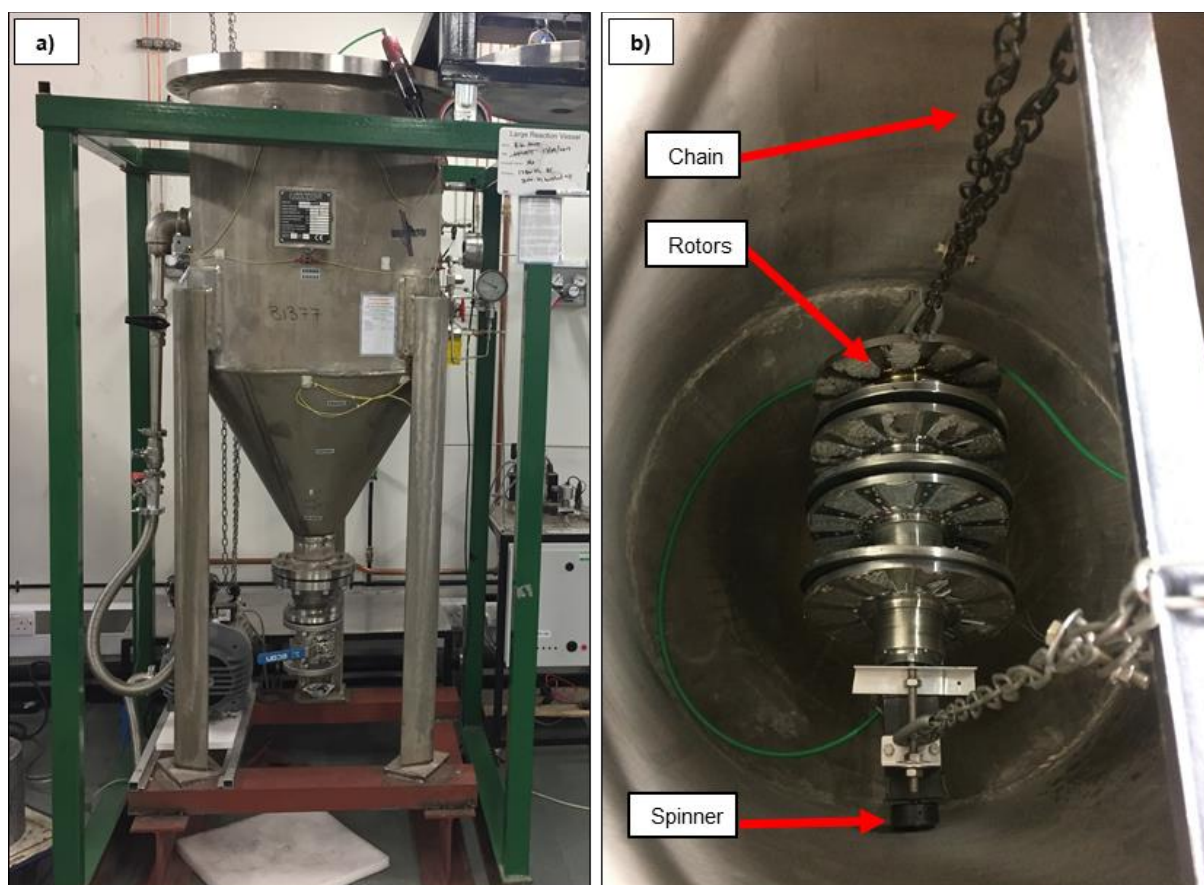159   transferred inertly to an argon-filled glovebox with oxygen level <10 ppm.

161   **Figure 2:** The 300 L reaction vessel used for HPMS processing, shown from the outside (a), and from the inside
162   (b) with the rotors loaded.

163   The sieving of the extracted powder was performed in 250 g batch sizes in an argon-filled

164   glovebox using a sieve stage with 2000 μm, 500 μm, 250 μm, 150 μm, 90 μm, and 45 μm

165   mesh size sieves (25 cm diameter) for 30 minutes. ICP-OES and carbon analysis was carried

166   out on the fraction of material that was remaining on every sieve and the fraction that had

167   passed through all of the sieves to identify any separation and removal of the epoxy coating.

168   **3.2.   Gravimetric Measurements of Hydrogen Absorption**

169   Gravimetric measurements of the hydrogen absorption were carried out on uncoated sintered

170   magnets with compositions $Nd_{31.1-x}Dy_xPr_{0.60}Fe_{64.78}Co_{3.00}Ga_{0.22}Cu_{0.15}Al_{0.15}$ (x=1.00 (composition

171   A), x=6.80 (B), x=8.45 wt.% (C), supplied by Magneti Ljubljana). These magnets were chosen

172   as they only differ in the Nd/Dy ratio so the effect of Dy could be investigated. The samples

173   were cut into cylinders of 3.65 mm diameter using an electrical discharge machine and ground

174 to 152 mg under an argon atmosphere where they were also stored. The samples were quickly
175 ground in air on each flat side before the measurements, to get the weight down to 150 g and
176 to keep the surface conditions constant. The gravimetric measurements of the hydrogen
177 decrepitation process were performed using an Intelligent Gravimetric Analyser (IGA-001)
178 from Hiden Isochema Ltd. The microbalance of the IGA has long-term stability of ±1 μg, a
179 weighing resolution of 0.2 g, and pressure resolution of ±0.02 %. After loading the samples,
180 the system was left open to air for a set time for air exposure (5, 30, and 60 minutes) to
181 determine the effect of oxidation after preparation of the rotors for the HPMS process and then
182 evacuated to 10^{-4} mbar pressure. Hydrogen was introduced at a rate of 200 mbar/minute to
183 the set pressure (1.2, 2.5, 5.0 or 10.0 bar), where it was held constant.

184

185 **3.3.   Analytical Methods**

186 A JEOL 7000 scanning electron microscope (SEM) was used for microstructural imaging of
187 the magnets, using a 20 kV accelerating voltage in backscattered mode, as well as
188 compositional analysis using energy-dispersive x-ray spectroscopy (EDX). Optical
189 microscopy, using a Laborlux 12HL microscope with Leitz lenses from 10x-100x, was used to
190 visually study the sieving fractions and the epoxy coating before and after thermal
191 demagnetisation treatments. Chemical analysis of the sieving fractions and starting magnets
192 was performed by Less Common Metals Ltd., using a Perkin Elmer Optima 5300
193 DV inductively coupled plasma optical emission spectrometer (ICP-OES). Carbon analysis
194 was performed by Magneti Ljubljana using an ELTRA CS-800, unless otherwise stated.

195 **4. Results and Discussion**

196 **4.1.   Extraction of NdFeB from Rotors Using Hydrogen**

197 Seven semi-embedded rotors and non-embedded rotors were processed separately in two
198 experiments. All the magnets in individual slots were scored in concentric circles using an
199 angle grinder to provide a fresh surface for the hydrogen, as shown in Figure 3, 15-30 minutes
200 before being loaded into the hydrogen vessel. The rotors were placed on a non-magnetic

201 metal rod, with wooden spacers between them so that the rotors would not stick together. The
202 rod was fastened to the top of the inside of the reactor with a chain, as shown in Figure 2b.
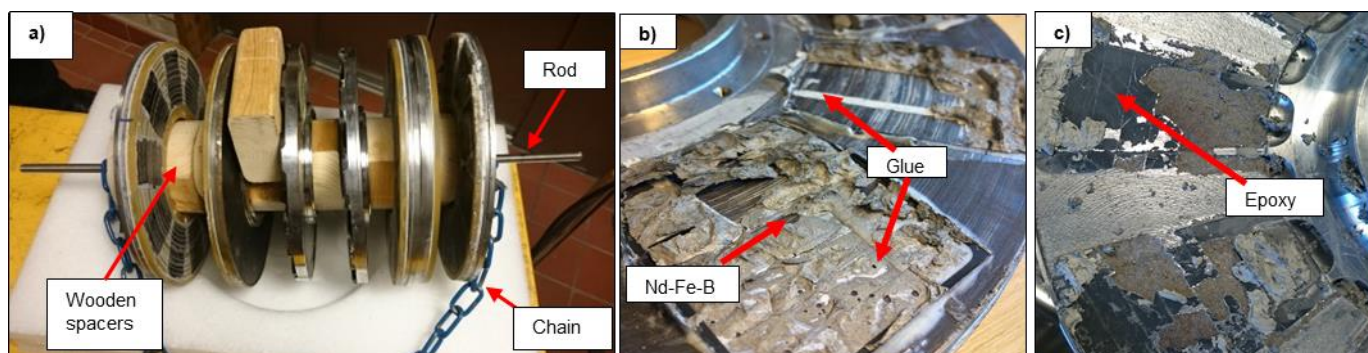
204 **Figure 3: A** non-embedded rotor scored, **a)** placed on a rod with wooden spacers. **b)** After hydrogen decrepitation
205 at 1.2-1.5 bar for 135 hours, some material was still left in the corners of some slots**.**

206 The hydrogen decrepitation was carried out at a pressure range of 1.2–1.5 bar, for a total
207 duration of 114 and 135 hours for the non-embedded and semi-embedded rotors, respectively.
208 The experiment was allowed to continue for such long time because the hydrogen pressure
209 was monitored throughout and the experiment was not ended until the pressure had been
210 stable for several hours. This was taken as indication that the reaction has completed. The
211 extraction was different between the semi- and non-embedded rotors. The semi-embedded
212 rotors were agitated using argon run pneumatic spinner after 18 hours of hydrogen exposure,
213 and it was observed from a small viewing window in the lid of the reactor that powder was
214 liberated from the assemblies. In the case of the non-embedded rotors, it was observed that
215 the powder self-liberated from the assemblies, so argon spinning was only carried towards the
216 end of the experiemnt to make sure all the powder was dropped into the collection pot.

217 **The yield was higher for the non-embedded rotors than for the semi-embedded rotors. The comparison**
218 **between the two rotors is given in**

220 Table 1. It was observed on the semi-embedded rotors that a small amount of the magnets
221 was still mechanically stuck in the bottom corners of the slots, as shown in Figure 3. The extent
222 of this would vary from rotor to rotor. However, for the non-embedded rotors, there was some
223 variation in the appearance of the rotors after exposure to hydrogen. Residues of glue and
224 epoxy, and sometimes magnet powder, was observed on some rotors, whereas there were
225 no residues in other cases. This is likely to be due to differences in how the magnets were

226 affixed to the rotors, and differences in surface materials on the rotor's ferritic stainless steel
227 base plate.

228

229

230 **Table 1: Comparison of the extraction of NdFeB from non-embedded and semi-embedded rotors. (* The**
231 **quoted yield includes a high degree of error because of the presence of epoxy and glue in the liberated**
232 **powder)**

Rotor type	Time (hours)	Yield (%)	Observation
Non-embedded	114	98*	A portion of powder self-liberated. Only a minor amount of powder remained on rotors.
Semi-embedded	135	92*	Chunks of un-liberated NdFeB mechanically stuck on rotors.

233

234 It was also observed that the non-embedded rotors reacted quicker than the semi-embedded
235 rotors, both with regards to the shorter reaction time, and a quicker drop in pressure in the
236 early phase of the reaction. It is possible that the embedding slows down the reaction, as it
237 hinders the volume expansion. The volume expansion is key in the decrepitation process, as
238 it leads to cracking (Moosa and Nutting, 1988), and as fracturing occurs this create fresh
239 surfaces for the reaction to propagate.

240 **4.2. Decontamination of Extracted Powders**

241 In order to recycle the extracted powder into new magnets, any auxiliary materials (glue,
242 plastic) and impurities must be removed. Work by Burkhardt et al., has shown that some
243 polymer coatings break up during processing and contaminate the final material, making it
244 unsuitable for reprocessing (Burkhardt et al., 2019). Work by Lopez et al., showed that
245 increases in carbon have an adverse impact on the final magnetic properties (Lopes et al.,
246 2012). This purification process will take place in an inert atmosphere to avoid oxidation of the
247 RE-rich phase. As already discussed in the literature review section 2, both oxygen and carbon

248   will have detrimental effects on the sintering process and magnetic properties of the recycled
249   magnets.

250   Chemical analysis of the extracted powder from the rotors showed an increased carbon
251   content in the extracted powder; 1750 ppm compared to 770 ppm in the base alloy, which is
252   explained by the observed adhesive residues. It was investigated whether sieving could
253   remove these impurities using the same process as for removing nickel from HDD scrap after
254   HPMS . A sieve stage with mesh sizes of 2000 µm, 500 µm, 250 µm, 150 µm, 90 µm and 45
255   µm was used. For the sieving trials, 250 g of powder was loaded the top mesh, and the
256   automatic shaker would agitate the sieves for 30 minutes until the experiment was ended. The
257   powder was collected from each mesh to be further analysed. As can be seen in Figure 4(a),
258   large chunks of glue and other binding materials were separated by the 2000 µm sieve.
259   However, the magnets' epoxy coating remained in all fractions, which was identified using
260   optical microscopy, see Figure 4 (b and c). The epoxy was present either on the surface of
261   the NdFeB powder particles or on its own in large flakes. The carbon content of each fraction
262   is plotted in Figure 4 (d), together with the weight fractions of hydrogenated powder remaining
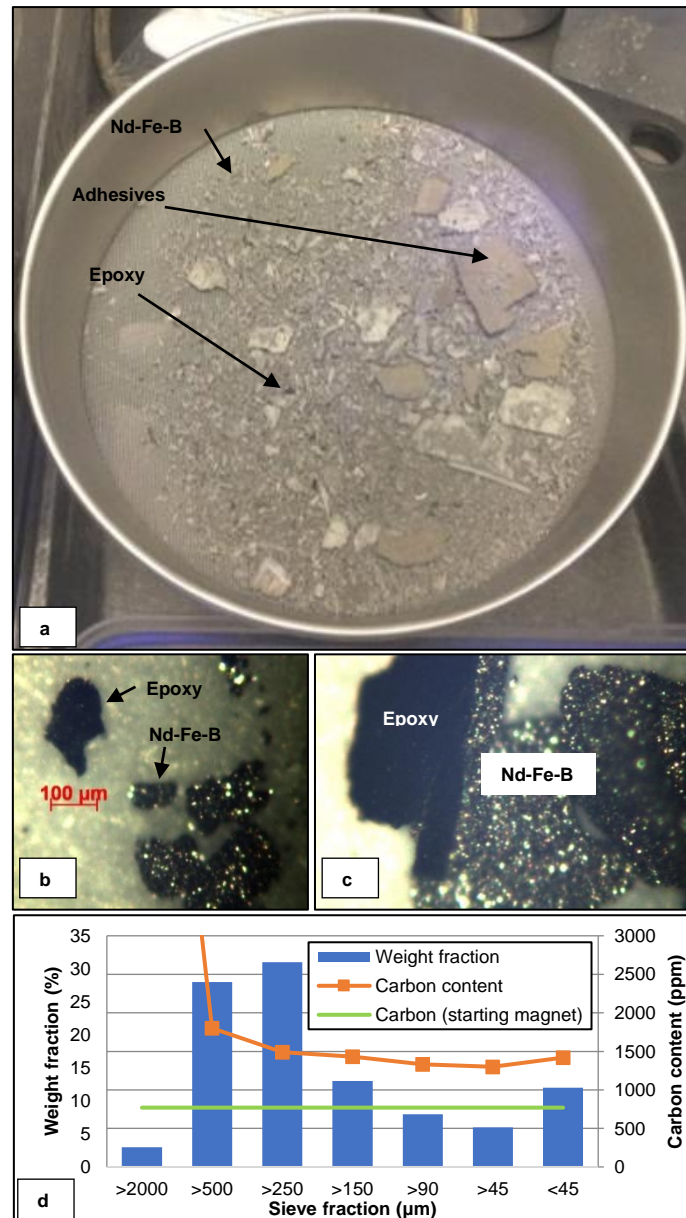263   in each sieve upon completion of the 30 minutes.

264

Figure 4: a) The residual impurities left on the 2000 μm sieve stage, however, all fractions contained epoxy from the coatings, either free (b) or on the NdFeB particles (c). This was reflected in the carbon analysis of each sieving fraction (d).

From the carbon analysis, it can be seen that even after sieving down to less than 45 μm the powder contains ~ 1500 ppm of carbon. From the work by Lopez et al., it can be seen that these levels of carbon would have an adverse impact on he magnetic properties of the magnets produced. The magnetic properties of the metal injection moulding (MIM) parts with carbon levels of 1500 ppm had inferior magnetic properties compared to those produced by conventional means with a carbon content of 600 ppm (Lopes et al., 2012).

4.3. Effect of Dy on the Kinetics of Hydrogen Decrepitation

275 Uncoated, sintered NdFeB magnets with three different Dy contents were exposed to
276 hydrogen. The Dy content of the magnet (A), (B) and (C) was 1.00wt.%, 6.8wt.% and
277 8.45wt.%, respectively. In the first set of experiments, each magnet composition was exposed
278 to three different lengths of air exposure times: 5, 30 and 60 minutes, before the system was
279 closed and evacuated. These time scales were selected to investigate how long damaged
280 magnets can be exposed to air for before hydrogen extraction takes place, or if the exposure
281 to air would inhibit the hydrogen absorption, as it has been shown that the RE-rich phase starts
282 to oxidise when exposed to air (Meakin et al., 2016).

283 All nine samples were cut into 3.65 mm diameter cylinders using an electrical discharge
284 machine and ground to 152 mg under an argon atmosphere where they were also stored. Just
285 before measurements were performed, the samples were quickly ground in the air on each
286 flat side, to get the weight down to 150 mg and to keep the surface conditions constant.

287 The absorption of hydrogen was then carried out at 1.2 bar hydrogen pressure and at room
288 temperature, which are typical processing conditions for the HPMS process, using an IGA.
289 The absorption traces for the 9 experiments are shown in Figure 5 and summarised in Table
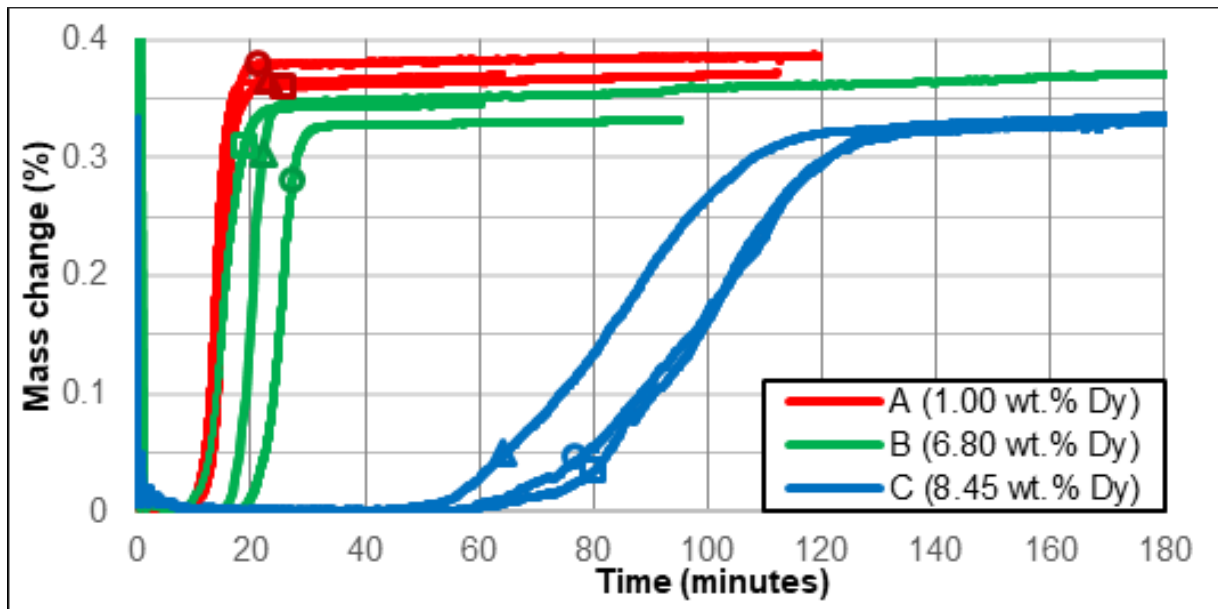290 2.

291

292 **Figure 5: Gravimetric measurements showing the mass change vs time during hydrogen decrepitation at**
293 **1.2 bar for magnets (A), (B) and (C), which only differ in Dy content.**

294 The initiation time refers to the time it takes from the start of the hydrogen pressure ramp (the
295 pressure ramp started at t=0 minute and reached 1.2 bar at approximately t=6 minutes) to the
296 start of the S-shaped curve. Saturation time refers to the time taken until the end of the S-

297 shaped curve, i.e. when the magnet is fully saturated with hydrogen and absorption is
298 complete. The absorption time is the time from initiation to saturation.

299 **Table 2: Summary of the gravimetric measurements at 1.2 bar hydrogen pressure.**

Sample name (wt.% Dy)	Air exposure (minutes)	Initiation time (minutes)	Saturation time (minutes)	Absorption time (minutes)	Hydrogen absorbed (wt.%)
A (1.00)	5	6.8	20.4	13.7	0.378
A (1.00)	30	8.1	18.6	10.5	0.363
A (1.00)	60	7.8	21.4	13.6	0.359
B (6.80)	5	13.7	27.0	13.3	0.346
B (6.80)	30	16.9	34.2	17.3	0.327
B (6.80)	60	7.8	24.3	16.5	0.342
C (8.45)	5	57.0	135.1	78.1	0.321
C (8.45)	30	42.0	121.9	79.9	0.322
C (8.45)	60	53.6	133.5	80.0	0.326
1.00: Avg. (SD)		7.6 (0.7)	20.1 (1.4)	12.6 (1.8)	0.367 (0.010)
6.80: Avg. (SD)		12.8 (4.6)	28.5 (5.1)	15.7 (2.1)	0.338 (0.010)
8.45: Avg. (SD)		50.9 (7.9)	130.2 (7.2)	79.3 (1.1)	0.323 (0.002)

300

301 From Figure 5 and Table 2, the following can be observed:

302 1. Varying the air exposure time between 5 and 60 minutes prior to hydrogen exposure
303 shows inconclusive results, this could be due to several factors including humidity.
304 Humidity has a big influence on the corrosion behaviour of sintered NdFeB (Yan et al.,
305 2009).

306 Saje et al., (1992) observed for the $Nd_{16-x}Dy_xFe_{76}B_8$ (x = 0-3) cast alloy; that air exposure
307 times between 5 and 1200 minutes led to a parabolic increase in initiation time for
308 hydrogen decrepitation at 1 bar pressure and 20 °C.

2. Increasing Dy content leads to delayed initiation of the hydrogen decrepitation reaction; it took on average 7.6 minutes for the magnet (A) to start reacting, 12.8 minutes for the magnet (B), and 50.9 minutes for the magnet (C).

3. Increasing Dy content leads to increased absorption time. On average, it took 12.6 minutes for the magnet (A), 15.7 minutes for the magnet (B) and 79.3 minutes for the magnet (C).

Hirano et al., (2006) have previously shown that Dy metal is more stable against hydrogenation than Nd. In their work, 1 g of pure Nd and Dy metal was individually exposed to 20 bar hydrogen at 273 K, and it was found that Dy had both delayed initiation and absorption times. The saturation time was 7 minutes and 830 minutes for Nd and Dy, respectively. This could explain point 2 and 3 above, as the hydrogen decrepitation reaction both initiates and propagates through the RE-rich grain boundaries. If these both initiate and react more slowly, this would lead to longer initiation and reaction times for the hydrogen decrepitation process as a whole. Furthermore, as the hydrogenation of the matrix phase is accommodated by the exothermic heat from the RE-hydride formation at the grain boundary (Harris et al., 1987), a slower reaction at the grain boundary could mean that the local temperature increase is lower, slowing down the diffusion of hydrogen into the matrix phase. However, Saje et al., (1992) did not see any effect of the Dy content on the hydrogen decrepitation kinetics of the $Nd_{16-x}Dy_xFe_{76}B_8$ (x = 0-3) cast alloy at 1 bar pressure at 20 °C. This could be explained by the higher RE content of approximately 35.1 wt.% in their work, compared to 31.1 wt.% in this work. With a higher amount of RE-rich phase, the effect of the Dy additions would be smaller as there would be a high amount of Nd present in this phase.

4. Increasing Dy content leads to less hydrogen being absorbed by the material: on average, magnet (A) absorbed 0.367 wt.% hydrogen, magnet (B) 0.338 wt.%, whereas magnet (C) absorbed 0.323 wt.% hydrogen.

This observation is supported by the work by Bartolomé et al., (1991), who showed that the $Dy_2Fe_{14}B$ phase absorbed less hydrogen than its Nd counterpart (Bartolomé et al., 1991). Furthermore, the volume expansion is lower for the Dy compound (3.5 vol.%) than the Nd compound (3.9 vol.%). The decrepitation reaction is based on the differential volume expansion of the matrix and grain boundary phases leading to inter- and trans-granular cracking, leading to pulverisation of the magnet (Moosa and Nutting, 1988). A lower volume expansion may affect the HPMS process with higher Dy contents will not break down to powder as efficiently as the low Dy content magnets, and hence why they

344 are more difficult to liberate from the assemblies after completion of the hydrogenation
345 reaction.

346 5. Magnet (C) absorbed hydrogen significantly slower than magnets (A) and magnet (B),
347 although the compositional differences between magnets (B) and magnet (C) are not
348 very large. The Dy content is larger in the RE-rich phase for the magnet (C) which
349 would slow down the reaction. However, the differences in the composition are much
350 larger between magnets (A) and magnet (B), and hence this result is confusing.

351 Harris et al., (1987) have shown that increased hydrogen pressure led to a decrease in both
352 initiation and saturation time for the $Nd_{15}Fe_{77}B_8$ cast alloy, following a logarithmic relation in
353 both cases. Higher hydrogen pressure could thus potentially be used to speed up the reaction
354 of the magnet (C), and the extraction of NdFeB from the rotors. In a subsequent set of
355 experiments, higher hydrogen pressures were applied to the magnet (C): 2.5 bar, 5 bar and
356 10 bar. Three runs were performed for every pressure, with 5 minutes of air exposure before
357 each run. The results are shown in Figure 6, where the absorption time is plotted versus
358 hydrogen pressure, and summarised in Table 3.

359 **Table 3: Summary of the gravimetric measurements of the magnet (C) at varying hydrogen pressure.**

Pressure (bar)	Air exposure (minutes)	Initiation time (minutes)	Saturation time (minutes)	Absorption time (minutes)	Amount absorbed (wt.%)
1.2	5	57.0	135.1	78.1	0.321
1.2	30	42.0	121.9	79.9	0.322
1.2	60	53.6	133.5	80.0	0.326
2.5	5	81.0	124.1	43.1	0.320
2.5	5	80.2	143.4	63.2	0.326
2.5	5	64.5	121.6	57.1	0.335
5.0	5	26.7	69.0	42.3	0.328
5.0	5	40.2	85.6	45.4	0.294
5.0	5	70.0	108.8	38.8	0.335
10.0	5	50.9	69.3	18.4	0.340
10.0	5	20.0	57.9	37.9	0.326
10.0	5	46.8	75.2	28.4	0.337
1.2: Avg. (SD)		50.9 (7.9)	130.2 (7.2)	79.2 (1.1)	0.323 (0.003)

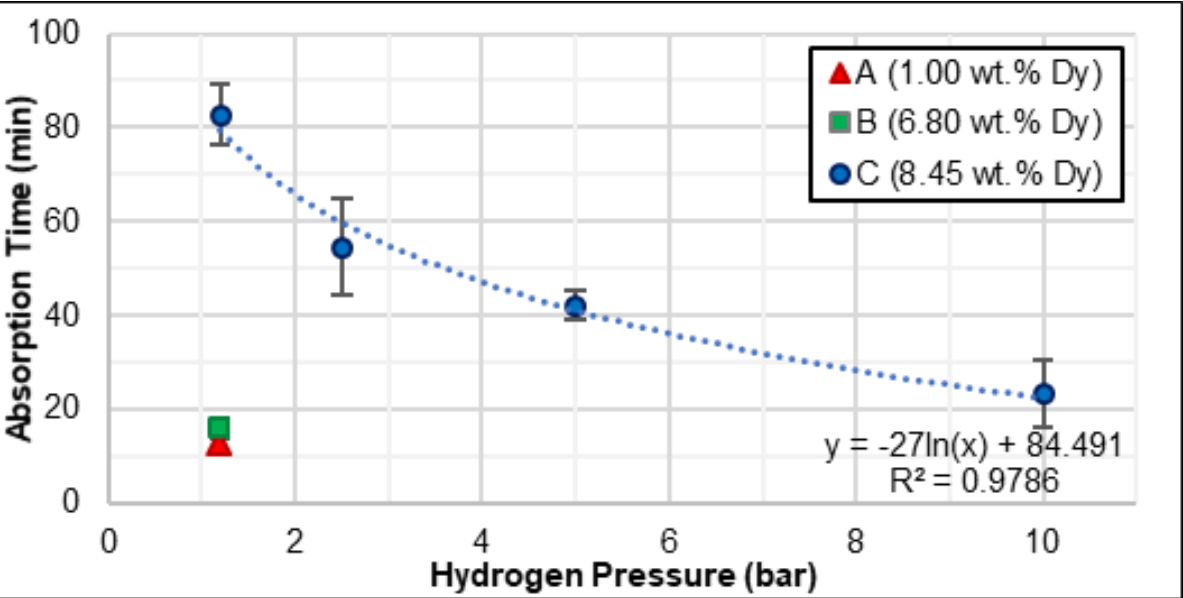|					
2.5: Avg. (SD)		75.2 (9.3)	129.7 (11.9)	50.5 (10.3)	0.327 (0.008)
5.0: Avg. (SD)		45.6 (22.2)	87.8 (20.0)	42.2 (14.1)	0.319 (0.003)
10.0: Avg. (SD)		39.3 (16.8)	67.5 (8.8)	28.2 (9.8)	0.334 (0.008)

360

361

Figure 6: Absorption time vs hydrogen pressure, generated from gravimetric measurements.

There is a clear decrease in absorption time with increasing pressure, which appears to follow a logarithmic relation very similar to what Harris et al., have shown for a $Nd_{16}Fe_{76}B_8$ cast alloy (Harris et al., 1987). However, there was no clear reduction in initiation time and the initiation data is inconclusive. Increasing the pressure from 1.2 bar to 5 bar and 10 bar, the absorption time decreased from 79 minutes to 42 and 28 minutes, respectively. This result means that it is likely that the extraction from the rotors could be significantly quicker by increasing the hydrogen pressure.

5. Conclusions

This paper is an early attempt at processing one particular design of automotive rotor and it is important to note that there are many different designs where the magnets are often more heavily embedded. However the data gathered and discussed in this paper can provide some initial information to help with design for recycling. For example if the systematic eco labelling outlined in the MaXycle project could be applied, then the composition of magnet would be known which would guide the process conditions for HPMS. Alternatively by choosing an appropriate binding material which does not break apart to the same extent on hydrogen

378 processing it would make the purification stage mush easier. This is a focus of the on-going
379 SUSMAGPRO project in the EU.

380 Furthermore, it is clear that a pre-treatment stage is required for the HPMS process, as is the
381 case with hard disk scrap, to initiate the reaction. Once the HPMS powder is generated then
382 in this case the epoxy-coating could not be entirely separated from the hydrogenated powder
383 with the technique used in this work. The carbon content was reduced from 1 % (10,000 ppm)
384 to 1490 ppm with a 250 µm sieve but on further fine sieving the carbon content was still at
385 1420 ppm, which is significantly higher than 770 ppm in the base alloy. It is not clear whether
386 different polymer coatings would interact in the same way and a much larger sample size of
387 drive motors would be required to investigate this. There may be a detrimental effect on the
388 magnetic properties of the recycled magnets if this powder was used to sinter magnets without
389 further purification, although it would require further work to confirm this. Further purification
390 methods need to be examined to reduce the carbon content down to acceptable levels as well
391 as choosing appropriate binding materials to avoid this.

392 The hydrogen decrepitation reaction was shown to be significantly slower for the rotor magnets
393 compared to lower Dy content magnets, which could be attributed both to the lower rare earth
394 content and higher Dy content of these magnets. Gravimetric measurements confirmed that
395 increasing Dy contents slows down absorption times, which has previously been unclear.
396 Therefore a higher pressure would be required to process automotive magnets. It is also
397 important to note that through time automotive magnets have been gradually decreasing in
398 Dy content.

408

References

Ahonen, S., Arvanitidis N., Auer A., Baillet, E., Bellato N., et al., Strengthening the European rare earths supply-chain Challenges and policy options A Report by the European rare earths competency network (ERECON). [Technical Report] European Commission. 2015. https://hal-cea.archives-ouvertes.fr/cea-01550114

Alonso, E., Wallington, T., Sherman, A., Everson, M. (2012). An Assessment of the Rare Earth Element Content of Conventional and Electric Vehicles," *SAE Int. J. Mater. Manf.* 5(2):473-477. https://doi.org/10.4271/2012-01-1061

Baba K, Nemoto T, Maruyama H, Taketani N, Itayagoshi K, Hirose Y. (2010). Hitachi's involvement in material resource recycling. Hitachi Rev 59(4): 180–187. www.hitachi.com/rev/pdf/2010/r2010_04_110.pdf

Baba, K., Hiroshige, Y., & Nemoto, T. (2013). Rare-earth magnet recycling. Hitachi Review, 62(8), 452–455. http://www.hitachi.com/rev/pdf/2013/r2013_08_105.pdf

Bartolomé, J., Luis, F., Fruchart, D., Isnard, O., Miraglia, S., Obbade, S., & Buschow, K.H.J. (1991). The effect of maximum hydrogenation on the $RE_2Fe_{14}X$, X = B,C compounds. Journal of Magnetism and Magnetic Materials, 101(1–3), 411–413. https://doi.org/10.1016/0304-8853(91)90798-F

Bast, U., Blank, R., Buchert, M., Elwert, T., Finsterwalder, F., Hörnig, G., Klier, T., Langkau, S., Marschneider-Weidemann, F., Müller, J. O., Thürigen, Ch., Treffer, F., & Walter, T. (2014). Recycling von Komponenten und Strategischen Metallen aus Elektrischen Fahrantrieben: MORE (Motor Recycling), Research Report. Publisher: Fraunhofer Institute http://publica.fraunhofer.de/dokumente/N-332362.html

Burkhardt, C., Lehmann, A., Podmiljsak, B., Kobe, S. (2020). A Systematic Classification and Labelling Approach to Support a Circular Economy Ecosystem for NdFeB-type Magnet. Unpublished work. Submitted to the Journal of Materials Science and Engineering A & B

Burkhardt, C., Lehmann, A., Frost, J., Podmiljsak, B., and Kobe, S. (2019). Enabling a circular economy ecosystem for NdFeB-type magnets: which measures are needed and what is really feasible? Conference proceedings of Sustainable industrial processing summit and exhibition. Paphos, Cyprus.

438 Dormidontov, N. A., Dormidontov, A. G., Lileev, A. S., Kamynin, A. V, & Lukin, A. A. (2017).
439 Effect of Partial Substitution of Neodymium with Praseodymium on the Magnetic and Process
440 Properties of Sintered Magnets of Type NdFeB, Metal Science and Heat Treatment, 58(9-10),
441 608-613. https://doi.org/10.1007/s11041-017-0064-6

442 Du, X., Graedel, T.E., 2011. Global Rare Earth In-Use Stocks in NdFeB Permanent Magnets.
443 J. Ind. Ecol. 15, 836–843. https://doi.org/10.1111/j.1530-9290.2011.00362.x

444 European Commission. (2014). Report on critical raw materials for the EU, Report of the Ad
445 hoc Working Group on defining critical raw materials. Retrieved from
446 http://ec.europa.eu/enterprise/policies/raw-materials/files/docs/crm-report-on-critical-raw-
447 materials_en.pdf

448 European Commission. (2017). Study on the review of the list of Critical Raw Materials
449 Criticality Assessments. https://doi.org/10.2873/876644

450 Falconnet, P. (1985). The economics of Rare Earths. Journal of the Less-Common Metals,
451 111, 9–15. http://dx.doi.org/10.1016/0022-5088(85)90163-8

452 Fidler, J. (1990). The Effect of Dopants (Al, Ga, Cu, Mo, V) on Microstructure and Coercivity
453 of Sintered $Nd_2Fe_{14}B$ Based Magnets. Proceedings of the 6th International Symposium on
454 Magnetic Anisotropy and Coercivity in Rare-Earth Transition Metal Alloys, Pittsburgh, USA,
455 176–180.

456 Gauder, D.R., Froning, M.H., White, R.J., Ray, A.E., 1988. Elevated temperature study of Nd-
457 Fe-B–based magnets with cobalt and dysprosium additions. J. Appl. Phys. 63, 3522–3524.
458 https://doi.org/10.1063/1.340729

459 Grieb, B., Pithan, C., Henig, E. T., & Petzow, G. (1991). Replacement of Nd by an intermetallic
460 phase in the intergranular region of Fe-Nd-B sintered magnets. Journal of Applied Physics,
461 70(10), 6354–6356. https://doi.org/10.1063/1.349940

462 Habib, K., Parajuly, K., & Wenzel, H. (2015). Tracking the Flow of Resources in Electronic
463 Waste - The Case of End-of-Life Computer Hard Disk Drives. Environmental Science and
464 Technology, 49(20), 12441–12449. https://doi.org/10.1021/acs.est.5b02264

465 Habib, K., & Wenzel, H. (2014). Exploring rare earths supply constraints for the emerging
466 clean energy technologies and the role of recycling. Journal of Cleaner Production, 84(1),
467 348–359. https://doi.org/10.1016/j.jclepro.2014.04.035

468 Harris, I. R., Mcguiness, P. J., Jones, D. G. R., & Abell, J. S. (1987). NdFeB Permanent
469 Magnets : Hydrogen Absorption / Desorption Studies (HADS) on $Nd_{16}Fe_{76}B_8$, and $Nd_2Fe_{14}B$,
470 Physica Scripta, T19. https://doi.org/435–440. 10.1088/0031-8949/1987/T19B/018

471 Hirano, K., Kadono, J., Yamamoto, S., Tanabe, T., & Miyake, H. (2006). Hydrogen-absorbing
472 characteristics of 15 rare earth elements. Journal of Alloys and Compounds, 408–412, 351–
473 354. https://doi.org/10.1016/j.jallcom.2005.04.052

474 Högberg, S., Holbøll, J., Mijatovic, N., Jensen, B. B., & Bendixen, F. B. (2017). Direct Reuse
475 of Rare Earth Permanent Magnets - Coating Integrity. IEEE Transactions on Magnetics, 53(4),
476 1-9. doi: 10.1109/TMAG.2016.2636804.

477 IEA, 2019. Global EV Outlook 2019. Paris.

478 Lopes, L. U., Carvalho, M. A., Chaves, R. S., Trevisan, M. P., Wendhausen, P. a. P., &
479 Takiishi, H. (2012). Study of Carbon Influence on Magnetic Properties of Metal Injection
480 Molding NdFeB Based Magnets. Materials Science Forum, 727–728, 124–129.
481 https://doi.org/10.4028/www.scientific.net/MSF.727-728.124

482 Malik Degri, (2014). The processing and characterisation of recycled NdFeB-type sintered
483 magnets. PhD Thesis. University of Birmingham.

484 MaXycle. (2018). A novel circular economy for sustainable RE-based magnets. EU Horizon
485 2020 funded project. http://www.maxycle.eu/ assessed on 27 July 2020. Project reference
486 number: ERA-MIN-2017_142.

487 Meakin, J. (2013). Targeted Hydrogen Decrepitation of NdFeB Magnets from Large
488 Commercial Assemblies. Master's Thesis. University of Birmingham.

489 Meakin, J. P., Speight, J. D., Sheridan, R. S., Bradshaw, A., Harris, I. R., Williams, A. J., &
490 Walton, A. (2016). 3-D Laser Confocal Microscopy Study of the Oxidation of NdFeB Magnets
491 in Atmospheric Conditions. Applied Surface Science, 378, 540–544.
492 https://doi.org/10.1016/j.apsusc.2016.03.182

493   Moosa, I. S., & Nutting, J. (1988). Hydrogen decrepitation of a permanent magnet NdFeB
494   alloy. Journal of The Less-Common Metals, 144(2), 221–225.
495   https://doi.org/10.1016/0022-5088(88)90135-X

496   Mottram, R. S., Davis, B., Yartys, V. A., & Harris, I. R. (2001). The use of metal hydride powder
497   blending in the production of NdFeB-type magnets. International Journal of Hydrogen Energy,
498   26(5), 441–448. https://doi.org/10.1016/S0360-3199(00)00076-8

499   Oesterreicher, K., & Oesterreicher, H. (1984). Structure and Magnetic Properties of
500    $Nd_2Fe_{14}BH_{2.7}$. Physica Status Solidi (a), 85(1), K61–K64.
501   https://doi.org/10.1002/pssa.2210850152

502   Reck, B. K., & Graedel, T. E. (2012). Challenges in Metal Recycling. Science, 337(2011), 690–
503   695. https://doi.org/10.1126/science.1217501

504   Sagawa, M., Fujimura, S., Yamamoto, H., Matsuura, Y., & Hirosawa, S. (1985). Magnetic
505   properties of rare-earth-iron-boron permanent magnet materials. Journal of Applied Physics,
506   57(8), 4094–4096. https://doi.org/10.1063/1.334629

507   Saje, B., Holc, J., & Beseničar, S. (1992). Hydrogenation process of Nd-Dy-Fe-B alloy. Journal
508   of Materials Science, 27(10), 2682–2686. https://doi.org/10.1007/BF00540690

509   Sasaki, T. T., Ohkubo, T., Une, Y., Kubo, H., Sagawa, M., & Hono, K. (2015). Effect of carbon
510   on the coercivity and microstructure in fine-grained NdFeB sintered magnet. Acta Materialia,
511   84, 506–514. https://doi.org/10.1016/j.actamat.2014.10.047

512   Schulze, R., & Buchert, M. (2016). Estimates of global REE recycling potentials from NdFeB
513   magnet material. Resources, Conservation and Recycling, 113, 12–27.
514   https://doi.org/10.1016/j.resconrec.2016.05.004

515   Sprecher, B., Xiao, Y., Walton, A., Speight, J., Harris, R., Kleijn, R., Visser, G., & Kramer, G.
516   J. (2014). Life cycle inventory of the production of rare earths and the subsequent production
517   of NdFeB rare earth permanent magnets. Environmental Science and Technology, 48(7),
518   3951–3958. https://doi.org/10.1021/es404596q

519   U.S. Department of Energy. (2011). U.S. Department of Energy: Critical materials strategy.
520   Retrieved from https://www.energy.gov/sites/prod/files/DOE_CMS2011_FINAL_Full.pdf

521 Walton, A., Yi, H., Rowson, N. A., Speight, J. D., Mann, V. S. J., Sheridan, R. S., Bradshaw,
522 A., Harris, I. R., & Williams, A. J. (2015). The use of hydrogen to separate and recycle
523 neodymium-iron-boron-type magnets from electronic waste. Journal of Cleaner Production,
524 104, 236–241. https://doi.org/10.1016/j.jclepro.2015.05.033

525 Yan, G., McGuiness, P., Farr, J., Harris, I.R. (2009) Environmental degradation of NdFeB
526 magnets, Journal of Alloys and Compounds. Volume 478, Issues 1–2, Pages 188-192,
527 https://doi.org/10.1016/j.jallcom.2008.11.153.

528 Zakotnik, M., Harris, I. R., & Williams, A. J. (2009). Multiple recycling of NdFeB-type sintered
529 magnets. Journal of Alloys and Compounds, 469(1–2), 314–321.
530 https://doi.org/10.1016/j.jallcom.2008.01.114